On the relation between optimal wideband matching and scattering of spherical waves

Nordebo, Sven; Bernland, Anders; Gustafsson, Mats; Sohl, Christian; Kristensson, Gerhard

2010

CODEN:LUTEDX/(TEAT-7204)/1-25/(2010)

On the relation between optimal wideband matching and scattering of spherical waves

Sven Nordebo, Anders Bernland, Mats Gustafsson, Christian Sohl, and Gerhard Kristensson

Electromagnetic Theory
Department of Electrical and Information Technology
Lund University
Sweden

Sven Nordebo
sven.nordebo@lnu.se

School of Computer Science, Physics and Mathematics
Linnaeus University
SE-351 95 Växjö
Sweden

Anders Bernland, Mats Gustafsson, Christian Sohl, and Gerhard Kristensson
{Anders.Bernland,Mats.Gustafsson,Christian.Sohl,Gerhard.Kristensson}@eit.lth.se

Department of Electrical and Information Technology
Electromagnetic Theory
Lund University
P.O. Box 118
SE-221 00 Lund
Sweden

Editor: Gerhard Kristensson

Abstract

Using an exact circuit analogy for the scattering of vector spherical waves, it is shown how the problem of determining the optimal scattering bounds for a homogeneous sphere in its high-contrast limit is identical to the closely related, and yet very different problem of finding the broadband tuning limits of the spherical waves. Using integral relations similar to Fano's broadband matching bounds, the optimal scattering limitations are determined by the static response as well as the high-frequency asymptotics of the reflection coefficient. The scattering view of the matching problem yields explicitly the necessary low-frequency asymptotics of the reflection coefficient that is used with Fano's broadband matching bounds for spherical waves, something that appears to be non-trivial to derive from the classical network point of view.

1 Introduction

Integral identities based on the properties of Herglotz functions [4], or positive real (PR) functions [35], constitute the basis for deriving Fano's broadband matching bounds [8] and have been used recently to describe a series of new sum rules for the scattering of electromagnetic waves [3, 4, 25, 26]. Hence, under the assumptions of linearity, continuity, time-translational invariance and passivity, sum rules can be derived from the analytic properties of the forward scattering dyadic, see *e.g.*, [25, 26], and have also applications in antenna theory, see *e.g.*, [11, 12, 24, 29, 30]. In [23], similar relations are used to determine the ultimate thickness to bandwidth ratio of radar absorbers. Limitations on the scattering of vector spherical waves have been considered in [3].

The sum rules rely on the well-known connection between the transfer functions of causal and passive systems and Herglotz functions, or positive real (PR) functions, as well as the analytic properties of these functions, see *e.g.*, [33, 35, 36]. Consequently, sum rules and limitations on arbitrary reflection coefficients stemming from passive systems can be derived, as described in [4]. The procedure is reviewed briefly in this paper.

By using Fano's approach, optimum broadband tuning limits of the higher-order spherical waves are considered in [29, 30], giving important physical insight into the matching limitations for UWB antennas, see also [9, 14, 15, 18, 31, 32, 34]. Previously, the Fano broadband matching bounds have been applied mainly to the lowest order spherical waves, and there is hence a need to further develop analytical results as an aid in the related numerical analysis. In [29, 30], it is conjectured that the low-frequency asymptotics of the positive real function $-\log\rho_{\tau l}$ is of the form

$$-\log(\pm\rho_{\tau l}) = 2\frac{a}{\mathrm{c}_0}s + 2(-1)^l(\frac{a}{\mathrm{c}_0})^{2l+1}c_{\tau l}s^{2l+1} + \cdots, \tag{1.1}$$

where $\rho_{\tau l}$ is the reflection coefficient corresponding to a TE ($\tau = 1$) or TM ($\tau = 2$) spherical wave of order l, s the Laplace variable, a the radius of a circumscribing sphere, c_0 the speed of light in free space, and $c_{\tau l}$ constants to be determined from network analysis and the circuit analogy of the spherical wave impedance.

In this contribution, an exact circuit analogy for the scattering of spherical waves is used similar to [6, 28], to show how the problem of determining the scattering limitations for a homogeneous sphere in its high-contrast limit becomes identical to the closely related, and yet very different problem of finding the broadband tuning limits of the spherical waves [29, 30]. Furthermore, the scattering view of the matching problem yields explicitly the necessary low-frequency asymptotics of the reflection coefficient (1.1), *i.e.*, the coefficients $c_{\tau l}$ that are used with Fano's broadband matching bounds for spherical waves. The coefficients $c_{\tau l}$ are given by the equation (4.17) in this paper. This is something that appears to be non-trivial to derive from the classical network point of view.

Optimal limitations for the scattering of spherical waves is considered where the geometry of the spherical object is known but the temporal dispersion is unknown. A detailed study of the high-frequency asymptotics of the reflection coefficient is performed including *e.g.*, the Debye and the Lorentz dispersion models, and is given in the Appendix. Using the integral relations derived in [4], which are similar to the relations in the derivation of Fano's broadband matching bounds [8], the optimal scattering limitations are determined by the static response as well as the high-frequency asymptotics of the reflection coefficient. As with the Fano approach, the integral relations yield a non-convex global optimization problem which in general is difficult to handle. As a numerical example, a relaxation of the Fano equations is considered here which is easily solved, and which is especially useful in the regime of Rayleigh scattering.

2 Limitations on passive reflection coefficients

This section reviews the general approach presented in [4] to find sum rules and physical limitations for reflection coefficients stemming from linear, continuous, time-translational invariant, and passive physical systems. The approach, which is used for the matching and scattering problems in the following sections, relies on the well-known connection between the transfer functions of causal and passive systems and Herglotz (or positive real) functions, as described in *e.g.*, [4, 33, 35, 36]. A set of integral identities for Herglotz functions was proved in [4]. Applied to a reflection coefficient ρ, they give a set of sum rules. The sum rules relate integrals of ρ over infinite frequency intervals to the static and high-frequency properties of the system, and so are much like Fano's matching equations. Physical limitations for the reflection coefficient are derived by considering finite frequency intervals. The general approach is presented in more detail in [4], where also all the necessary proofs are given.

2.1 Herglotz functions and integral identities

Here the class of Herglotz functions is reviewed briefly, and the integral identities used to obtain sum rules and limitations for reflection coefficients are presented. A Herglotz function $h(z)$ is defined as an analytic function for $z \in \mathbb{C}_+ = \{z : \operatorname{Im} z > 0\}$

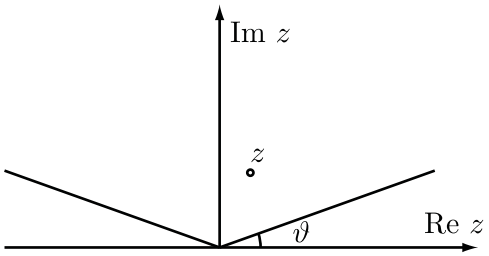

Figure 1: The cone $\{z : \vartheta \leq \arg z \leq \pi - \vartheta\}$ for some $\vartheta \in (0, \pi/2]$.

with the property that $\operatorname{Im} h(z) \geq 0$, *cf.*, [4, 20]. It is assumed that h obeys the symmetry

$$h(z) = -h^*(-z^*) \tag{2.1}$$

where $(\cdot)^*$ denotes the complex conjugate [4]. Herglotz functions stemming from reflection coefficients in real physical systems exhibit this symmetry property [33, 35, 36]. For all Herglotz functions it holds that $\lim_{z\hat{\to}0} zh(z) = a_{-1} \leq 0$ and $\lim_{z\hat{\to}\infty} h(z)/z = b_1 \geq 0$. Throughout this paper, $z\hat{\to}0$ means $|z| \to 0$ in the cone $\vartheta \leq \arg z \leq \pi - \vartheta$ for any $\vartheta \in (0, \pi/2]$, and likewise for $z\hat{\to}\infty$, see Figure 1.

It is assumed that the low- and high-frequency asymptotic expansions are given by

$$\begin{cases} h(z) = \displaystyle\sum_{m=0}^{N} a_{2m-1} z^{2m-1} + o(z^{2N-1}) \quad \text{as } z\hat{\to}0 \\ h(z) = \displaystyle\sum_{m=0}^{M} b_{1-2m} z^{1-2m} + o(z^{1-2M}) \quad \text{as } z\hat{\to}\infty, \end{cases} \tag{2.2}$$

where the little ordo notation o is defined as in [21], and M and N are non-negative integers (or possibly infinity), chosen so that all the coefficients a_m and b_m are real valued, and hence that all the even indexed coefficients are zero [4]. The asymptotic expansions are clearly valid as $z \to 0$ ($z \to \infty$) for any argument in the case h is analytic in a neighbourhood of the origin (infinity).

The following integral identities have been derived in [4], and they are the starting point to derive limitations on reflection coefficients:

$$\frac{2}{\pi} \int_0^\infty \frac{\operatorname{Im} h(x)}{x^{2p}} \, \mathrm{d}x = a_{2p-1} - b_{2p-1}, \quad \text{for } p = 1 - M, 2 - M, \ldots, N. \tag{2.3}$$

It should be noted that the integral identities in (2.3) do not apply in the case when the largest possible integers N and M are $N = M = 0$ in (2.2). In case the imaginary part $\operatorname{Im} h(x)$ is not regular on the real axis, the integral should be interpreted as

$$\lim_{\varepsilon\to0^+} \lim_{y\to0^+} \frac{2}{\pi} \int_{\varepsilon<|x|<\varepsilon^{-1}} \frac{\operatorname{Im} h(x + \mathrm{i}y)}{x^{2p}} \, \mathrm{d}x = a_{2p-1} - b_{2p-1}, \tag{2.4}$$

for $p = 1 - M, 2 - M, \ldots, N$, and where i denotes the imaginary unit, $\mathrm{i}^2 = -1$. This is equivalent to interpreting (2.3) in the distributional sense [4]. Equation

(2.3) is assumed to be replaced by (2.4) whenever necessary throughout this paper. The identities (2.3) can be used to derive Fano's matching equations [8]. They have also been used recently to derive a series of new sum rules for the scattering of electromagnetic waves [3, 25, 26], with applications in antenna theory [11, 29, 30]. There are other applications for the identities (2.3) as well, see *e.g.*, [5, 10, 13, 16, 23].

2.2 Limitations on passive reflection coefficients

Let $\rho(\omega)$ denote a reflection coefficient of a system where the reflected signal $u(\omega)$ is related to the incoming signal $v(\omega)$ as

$$u(\omega) = \rho(\omega)v(\omega),$$

where ω is the angular frequency. It is assumed that the reflection coefficient is the Fourier transform of a real valued convolution kernel $\rho_{\rm r}(t)$. The Fourier transform is defined as $\rho(\omega) = \int_{-\infty}^{\infty} \rho_{\rm r}(t) {\rm e}^{{\rm i}\omega t}\,{\rm d}t$ when $\rho_{\rm r}(t)$ is sufficiently regular, and it is otherwise defined in the appropriate distributional sense [4, 36].

If $\rho(\omega)$ corresponds to a passive system, it is bounded with $|\rho(\omega)| \leq 1$. The system is causal if the reflection coefficient corresponds to a causal convolution kernel $\rho_{\rm r}^{\rm c}(t)$ which vanishes for $t < 0$. It is a well-known result that the reflection coefficient $\rho^{\rm c}(\omega)$ of a passive and causal system is an analytic function bounded in magnitude by one in the open upper half plane, *i.e.*, $\rho^{\rm c}(\omega+{\rm i}\sigma)$ is analytic and $|\rho^{\rm c}(\omega+{\rm i}\sigma)| \leq 1$ for $\sigma > 0$ [33, 35]. For a non-causal system (consider *e.g.*, the scattering of electromagnetic waves [3, 20]), introduce a time delay t_0 so that ${\rm e}^{{\rm i}\omega t_0}\rho(\omega)$ corresponds to a causal convolution kernel $\rho_{\rm r}(t-t_0)$. The reflection coefficient $\rho(\omega+{\rm i}\sigma)$ is thus an analytic function for $\sigma > 0$, and it is bounded according to $|{\rm e}^{({\rm i}\omega-\sigma)t_0}\rho(\omega+{\rm i}\sigma)| \leq 1$.

A Herglotz function can be constructed by taking the complex logarithm of ρ [4]. It requires that the zeros of ρ are removed, which is done with a Blaschke-product [7]. The Herglotz function is therefore (with $z = \omega + {\rm i}\sigma$):

$$h(z) = -{\rm i}\log\left({\rm e}^{{\rm i}zt_0}\rho(z)\prod_n \frac{1-z/z_n^*}{1-z/z_n}\right), \tag{2.5}$$

where the zeros z_n of ρ in $\mathbb{C}^+$ are repeated according to their multiplicity. The convolution kernel $\rho_{\rm r}(t)$ is real-valued, and so $\rho({\rm i}\sigma)$ is real valued on the imaginary axis with the symmetry $\rho(z) = \rho^*(-z^*)$ for $z \in \mathbb{C}^+$. Without loss of generality it may be assumed that $\rho({\rm i}\sigma) > 0$, in which case $h(z)$ obeys the symmetry (2.1). If $\rho({\rm i}\sigma) < 0$, consider the function $-\rho(z)$ instead.

Suppose that the low-frequency asymptotics of $-{\rm i}\log\rho(z)$ is given by $-{\rm i}\log\rho(z) = \sum_{m=0}^{N} a_{2m-1}^{(0)} z^{2m-1} + o(z^{2N-1})$ as $z \hat{\to} 0$. The low-frequency asymptotics of $h(z)$ is then

$$h(z) = zt_0 + \sum_{m=0}^{N} a_{2m-1}^{(0)} z^{2m-1} + o(z^{2N-1}) + \sum_{m=1,3,\ldots}^{\infty} \frac{2}{m} \sum_n {\rm Im}\left\{\frac{1}{z_n^m}\right\} z^m, \quad \text{as } z \hat{\to} 0. \tag{2.6}$$

Note that there are only odd indices m in the last summation above since the complex zeros appear in symmetric pairs $(z_n, -z_n^*)$.

With $p = 1, 2, \ldots, N$, the following relationships are now obtained from (2.3):

$$\frac{2}{\pi}\int_0^\infty \frac{1}{\omega^{2p}} \log|\rho(\omega)|^{-1}\,\mathrm{d}\omega = \left\{ \delta_{p1}(t_0 - b_1) + a_{2p-1}^{(0)} + \frac{2}{2p-1}\sum_n \mathrm{Im}\left\{\frac{1}{z_n^{2p-1}}\right\}\right\}. \tag{2.7}$$

Here δ_{p1} denotes the Kronecker delta. Note that the term $b_1 \geq 0$ originates from the high-frequency asymptotics.

Denote $\rho_0 = \max_\omega |\rho(\omega)|$ where the maximum is taken over the angular frequency interval $\omega \in [\omega_0(1 - \frac{B}{2}), \omega_0(1 + \frac{B}{2})]$, ω_0 is the center angular frequency and B the relative bandwidth ($0 \leq B \leq 2$). The integral identities (2.7) then yield the following inequalities:

$$\begin{aligned}\log \rho_0^{-1} B \leq \log \rho_0^{-1} G_p(B) &\leq \omega_0^{2p-1}\int_0^\infty \frac{1}{\omega^{2p}} \log|\rho(\omega)|^{-1}\,\mathrm{d}\omega \\ &= \frac{\pi}{2}\left[\delta_{p1} t_0 \omega_0^{2p-1} + a_{2p-1}^{(0)}\omega_0^{2p-1} + \frac{2}{2p-1}\sum_n \mathrm{Im}\left\{\left(\frac{\omega_0}{z_n}\right)^{2p-1}\right\}\right], \end{aligned} \tag{2.8}$$

where it has been used that $b_1 \geq 0$. The factor $G_p(B)$ is defined by

$$G_p(B) = \int_{1-B/2}^{1+B/2} \frac{1}{x^{2p}}\,\mathrm{d}x = \frac{1}{2p-1}\frac{(1+\frac{B}{2})^{2p-1} - (1-\frac{B}{2})^{2p-1}}{(1-\frac{B^2}{4})^{2p-1}}. \tag{2.9}$$

Note that $B \leq G_p(B)$ for all $0 \leq B \leq 2$, and $G_p(B) \approx B$ in the narrowband approximation when $B \ll 1$.

2.3 Fano broadband matching bounds for spherical waves

The classical broadband matching bounds for lossless networks by Fano [8] are revisited using the Herglotz function formulation and integral identities (2.3) and (2.7). The Fano matching bounds are then used to formulate the problem of finding the broadband tuning limits of the wave impedance of the spherical waves as in [29, 30].

In circuit theory it is convenient to employ the Laplace variable $s = -\mathrm{i}z = \mathrm{j}\omega + \sigma$, with $\mathrm{j} = -\mathrm{i}$. The Herglotz function $h(z)$ then corresponds to a positive real (PR) function $g(s) = -\mathrm{i}h(z)$ with the property that $g(s)$ is analytic with $\mathrm{Re}\, g(s) \geq 0$ for $\mathrm{Re}\, s = \sigma > 0$, *cf.*, [22,36]. The symmetry (2.1) takes the form $g(s) = g^*(s^*)$. The low- and high-frequency asymptotics are given by

$$\begin{cases} g(s) = \displaystyle\sum_{m=0}^{N} A_{2m-1} s^{2m-1} + o(s^{2N-1}) \quad \text{as } \mathrm{i}s \hat{\to} 0 \\ g(s) = \displaystyle\sum_{m=0}^{M} B_{1-2m} s^{1-2m} + o(s^{1-2M}) \quad \text{as } \mathrm{i}s \hat{\to} \infty, \end{cases} \tag{2.10}$$

where all coefficients are real valued and the even indexed coefficients are zero. Furthermore, the PR function property implies that $A_{-1} \geq 0$ and $B_1 \geq 0$. Note

also that the mapping $g(s) = -\mathrm{i}h(\mathrm{i}s)$ implies the relations $A_{2m-1} = (-1)^{m+1}a_{2m-1}$ and $B_{2m-1} = (-1)^{m+1}b_{2m-1}$ for the coefficients in (2.2) and (2.10). The following integral identity now follows directly from (2.3):

$$\frac{2}{\pi}\int_0^\infty \frac{\operatorname{Re} g(\mathrm{j}\omega)}{\omega^{2p}}\,\mathrm{d}\omega = (-1)^{p+1}\left(A_{2p-1} - B_{2p-1}\right), \quad \text{for } p = 1-M, 2-M, \ldots, N. \tag{2.11}$$

Let $\rho(s)$ denote the reflection coefficient corresponding to an arbitrary impedance function defined by a passive RLC network. Such an impedance function can always be represented by a lossless two-port which is terminated in a pure resistance [8]. The appropriate PR function corresponding to (2.5) is given by

$$g(s) = -\log\left(\rho(s)\prod_n \frac{1+s/s_n^*}{1-s/s_n}\right), \tag{2.12}$$

where s_n are the zeros of $\rho(s)$ with $\operatorname{Re} s_n > 0$. Note that the causality factor $\mathrm{e}^{\mathrm{i}zt_0}$ is not needed here, since the reflection coefficient corresponds to a causal convolution kernel.

Suppose that the low-frequency asymptotics of $-\log\rho(s)$ is given by $-\log\rho(s) = \sum_{m=0}^{M} A_{2m-1}^{(0)} s^{2m-1} + o(s^{2M-1})$, as $\mathrm{i}s \hat{\to} 0$. The low-frequency asymptotics of $g(s)$ is then given by

$$g(s) = \sum_{m=0}^{N} A_{2m-1}^{(0)} s^{2m-1} + o(s^{2N-1}) - \sum_{m=1,3,\ldots}^{\infty} \frac{2}{m}\sum_n \operatorname{Re}\left\{\frac{1}{s_n^m}\right\} s^m, \quad \text{as } \mathrm{i}s \hat{\to} 0. \tag{2.13}$$

With $p = 1, 2, \ldots, N$, the following relationships are now obtained from (2.11) (*cf.*, [8]):

$$\frac{2}{\pi}\int_0^\infty \frac{1}{\omega^{2p}} \log|\rho(\mathrm{j}\omega)|^{-1}\,\mathrm{d}\omega = (-1)^{p+1}\left\{A_{2p-1}^{(0)} - \delta_{p1}B_1 - \frac{2}{2p-1}\sum_n \operatorname{Re}\left\{\frac{1}{s_n^{2p-1}}\right\}\right\}. \tag{2.14}$$

Note that $B_1 = 0$ if the circuit consists of only lumped elements, since $\rho(s)$ is a rational function in this case. Furthermore, for rational functions $\rho(s)$ the asymptotic expansions (2.10) are valid as $s \to 0$ and $s \to \infty$, respectively.

Consider now the broadband matching problem as described in [8]. In Figure 2 is shown the cascade of two lossless and reciprocal two-ports N' and N'' with a source at one side and a resistive termination at the other side. Let N' be the fixed network and N'' the matching network. The reflection and transmission coefficients for the overall two-port are denoted by ρ_1, ρ_2 and ϱ. Since the overall two-port is lossless with $|\rho_1|^2 = 1 - |\varrho|^2 = |\rho_2|^2$, the optimal matching limitations for the input port of interest with coefficient ρ_2 may be conveniently analyzed by considering the opposite port with coefficient ρ_1, as depicted in Figure 2.

The reflection coefficient ρ_1 for the overall two-port is given by

$$\rho_1 = \rho_1' + \frac{\varrho'^2\rho_1''}{1-\rho_2'\rho_1''}. \tag{2.15}$$

Without loss of generality, it may be assumed that $\rho_1'(0) = 1$ (where $s = 0$). Furthermore, it is also assumed that $\rho_2'(0)\rho_1''(0) = -1$ so that there is no cancellation of zeros at $s = 0$ in (2.15). This condition is easily achieved by choosing the appropriate LC ladder structure for N'' if $\rho_2'(0)$ is known, *cf.*, also [8].

Suppose that the transmission coefficient ϱ' has a zero of order N at $s = 0$. This implies that $\rho_1'(s)\rho_1'(-s) = 1 - \varrho'(s)\varrho'(-s) = 1 + \mathcal{O}(s^{2N})$, where the big ordo notation $\mathcal{O}$ is defined as in [21]. Suppose further that the low-frequency asymptotics of ρ_1' is given by $-\log \rho_1'(s) = \sum_{m=0}^{\infty} A_m^{(0)\prime} s^m$ as $s \to 0$. Hence,

$$-\log \rho_1'(s) - \log \rho_1'(-s) = \sum_{m=0}^{\infty} A_m^{(0)\prime} s^m + \sum_{m=0}^{\infty} A_m^{(0)\prime} (-1)^m s^m = \mathcal{O}(s^{2N}), \quad \text{as } s \to 0, \tag{2.16}$$

implying that $A_m^{(0)} = A_m^{(0)\prime} = 0$ for $m = 0, 2, \ldots, 2N-2$. Furthermore, from (2.15) follows that $\frac{\partial^m}{\partial s^m} \log \rho_1|_{s=0} = \frac{\partial^m}{\partial s^m} \log \rho_1'|_{s=0}$ for $0 \leq m \leq 2N-1$, and hence the invariance of the Taylor coefficients $A_m^{(0)} = A_m^{(0)\prime}$ for $m = 1, 3, \ldots, 2N-1$. Thus, (2.14) can now be applied with $A_{2p-1}^{(0)} = A_{2p-1}^{(0)\prime}$ for $p = 1, 2, \ldots, N$. These are the original Fano matching equations formulated in [8].

Consider now the problem of finding the optimum broadband tuning limits of the wave impedance of the spherical waves, as described in *e.g.*, [29, 30]. Hence, consider the matching problem of an outgoing TE_l ($\tau = 1$) or TM_l ($\tau = 2$) spherical wave of order l. As was shown by Chu [6], the wave impedance of the spherical waves as seen at a spherical boundary can be represented by a finite LC high-pass ladder network terminated in a fixed resistance, *cf.*, Figure 3. The impedance $Z_{\tau l}$ is the normalized wave impedance as seen at a spherical boundary of radius a, *i.e.*, at the left (antenna) side of the equivalent circuit in Figure 3. The input impedance used in the Fano analysis is the impedance $Z_{1,\tau l}$ as seen from the opposite, right-hand side of the equivalent circuit when it is correctly terminated in a pure resistance. The corresponding reflection coefficient is given by $\rho_{1,\tau l} = (Z_{1,\tau l} - 1)/(Z_{1,\tau l} + 1)$.

It has been conjectured [29, 30] that the low-frequency asymptotics of $-\log \rho_{1,\tau l}$ is of the form

$$-\log(\pm\rho_{1,\tau l}) = A_1^{(0)} s + A_{2l+1}^{(0)} s^{2l+1} + \mathcal{O}(s^{2l+2}), \quad \text{as } s \to 0 \tag{2.17}$$

where

$$\begin{cases} A_1^{(0)} = 2\dfrac{a}{\mathrm{c}_0} \\ A_{2l+1}^{(0)} = 2(-1)^l (\dfrac{a}{\mathrm{c}_0})^{2l+1} c_{\tau l} \end{cases} \tag{2.18}$$

and where $c_{\tau l}$ is a constant determined from network analysis.

The conjecture (2.18) may be verified by using the equivalent circuits for a fixed order $l = 1, 2, \ldots$. However, from a network (N') analysis point of view, it seem to be non-trivial to prove it for general order l. In the next two sections, it is shown that the conjecture (2.18) is true and an explicit expression for $A_{2l+1}^{(0)}$ is given by showing that the matching problem is equivalent to the problem of finding the optimal scattering limitations for a homogeneous sphere in its high-contrast limit, *i.e.*, in the limit as the permittivity or the permeability tends to infinity.

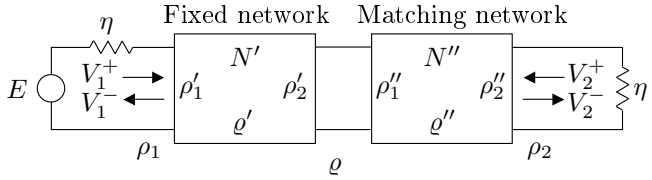

Figure 2: Cascade of two reciprocal two-ports N' and N''. Here, ρ_1, ρ_2 and ϱ denote the overall scattering parameters.

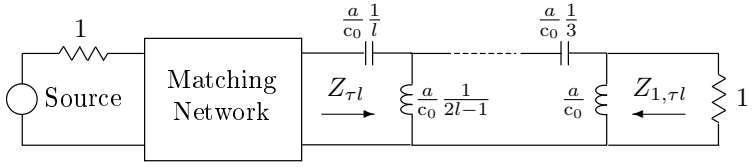

Figure 3: Matching network and equivalent circuit for the impedance of a TM_l wave at a spherical boundary of radius a. The circuit is drawn for a TM_l wave of odd order l.

3 Optimal limitations for scattering of vector spherical waves

Consider the scattering of vector spherical waves which is associated with an isotropic and homogeneous sphere of radius a, and with relative permeability and permittivity μ and ϵ, respectively. The refractive index is $n = (\mu\epsilon)^{1/2}$ and the relative wave impedance $\eta = (\mu/\epsilon)^{1/2}$. The exterior of the sphere is free space, and c_0 and η_0 are the speed of light and the wave impedance of free space, respectively. For convenience, introduce the angular wave number $\mathrm{Re}\{k\} = \omega/\mathrm{c}_0$. Allow k to take values in the upper-half plane, so that k corresponds to z/c_0 in Section 2.2. Let (r, θ, ϕ) denote the spherical coordinates and $\boldsymbol{r} = r\hat{\boldsymbol{r}}$ the corresponding radius vector.

3.1 Exterior of the sphere

The electric and magnetic fields outside the sphere, *i.e.*, for $r \geq a$, are given by

$$\boldsymbol{E}(\boldsymbol{r}) = \sum_{l=1}^{\infty}\sum_{m=-l}^{l}\sum_{\tau=1}^{2} a_{\tau ml}^{(1)}\boldsymbol{u}_{\tau ml}^{(1)}(k\boldsymbol{r}) + a_{\tau ml}^{(2)}\boldsymbol{u}_{\tau ml}^{(2)}(k\boldsymbol{r}) \tag{3.1}$$

$$\boldsymbol{H}(\boldsymbol{r}) = \frac{1}{\mathrm{i}\eta_0}\sum_{l=1}^{\infty}\sum_{m=-l}^{l}\sum_{\tau=1}^{2} a_{\tau ml}^{(1)}\boldsymbol{u}_{\bar{\tau} ml}^{(1)}(k\boldsymbol{r}) + a_{\tau ml}^{(2)}\boldsymbol{u}_{\bar{\tau} ml}^{(2)}(k\boldsymbol{r}) \tag{3.2}$$

where $\boldsymbol{u}_{\tau ml}^{(1)}(k\boldsymbol{r})$ and $\boldsymbol{u}_{\tau ml}^{(2)}(k\boldsymbol{r})$ are *outgoing* and *incoming* vector spherical waves, respectively, see *e.g.*, [2, 17, 19], and $a_{\tau ml}^{(j)}$ the corresponding multipole coefficients. Here $\tau = 1$ corresponds to transverse electric (TE) waves, $\tau = 2$ corresponds to

transverse magnetic (TM) waves, and $\bar{\tau} = 3 - \tau$ denotes the complimentary index. The other indices are $l = 1, 2, \ldots$, and $m = -l, -l+1, \ldots, l$, where l denotes the *order* of the spherical wave. The vector spherical waves are given by

$$\boldsymbol{u}_{1ml}^{(j)}(k\boldsymbol{r}) = \mathrm{h}_l^{(j)}(kr)\boldsymbol{A}_{1ml}(\hat{\boldsymbol{r}}) \tag{3.3}$$

$$\boldsymbol{u}_{2ml}^{(j)}(k\boldsymbol{r}) = \frac{(kr\mathrm{h}_l^{(j)}(kr))'}{kr}\boldsymbol{A}_{2ml}(\hat{\boldsymbol{r}}) + \sqrt{l(l+1)}\frac{\mathrm{h}_l^{(j)}(kr)}{kr}\boldsymbol{A}_{3ml}(\hat{\boldsymbol{r}}) \tag{3.4}$$

where $\boldsymbol{A}_{\tau ml}(\hat{\boldsymbol{r}})$ are the *vector spherical harmonics* and $\mathrm{h}_l^{(j)}(x)$ the *spherical Hankel* functions of the jth kind, $j = 1, 2$, and order l, see *e.g.*, [2, 17, 19]. Here, $(\cdot)'$ denotes differentiation with respect to the argument kr. The vector spherical harmonics $\boldsymbol{A}_{\tau ml}(\hat{\boldsymbol{r}})$ are given by

$$\begin{cases} \boldsymbol{A}_{1ml}(\hat{\boldsymbol{r}}) = \dfrac{1}{\sqrt{l(l+1)}}\nabla \times (\boldsymbol{r}\mathrm{Y}_{ml}(\hat{\boldsymbol{r}})) \\ \boldsymbol{A}_{2ml}(\hat{\boldsymbol{r}}) = \hat{\boldsymbol{r}} \times \boldsymbol{A}_{1ml}(\hat{\boldsymbol{r}}) \\ \boldsymbol{A}_{3ml}(\hat{\boldsymbol{r}}) = \hat{\boldsymbol{r}}\mathrm{Y}_{ml}(\hat{\boldsymbol{r}}) \end{cases} \tag{3.5}$$

where $\mathrm{Y}_{ml}(\hat{\boldsymbol{r}})$ are the scalar *spherical harmonics* given by

$$\mathrm{Y}_{ml}(\theta, \phi) = (-1)^m \sqrt{\frac{2l+1}{4\pi}}\sqrt{\frac{(l-m)!}{(l+m)!}}\mathrm{P}_l^m(\cos\theta)\mathrm{e}^{\mathrm{i}m\phi}, \tag{3.6}$$

and where $\mathrm{P}_l^m(x)$ are the *Associated Legendre functions*, see *e.g.*, [2]. The vector spherical harmonics $\boldsymbol{A}_{\tau ml}(\hat{\boldsymbol{r}})$ are orthonormal on the unit sphere and have the directional properties $\hat{\boldsymbol{r}} \cdot \boldsymbol{A}_{\tau ml}(\hat{\boldsymbol{r}}) = 0$ for $\tau = 1, 2$ and $\hat{\boldsymbol{r}} \times \boldsymbol{A}_{3ml}(\hat{\boldsymbol{r}}) = \boldsymbol{0}$.

3.2 Interior of the sphere and scattering coefficients

The electric and magnetic fields inside the sphere for $r \leq a$ are given by

$$\boldsymbol{E}(\boldsymbol{r}) = \sum_{l=1}^{\infty}\sum_{m=-l}^{l}\sum_{\tau=1}^{2} b_{\tau ml}\boldsymbol{v}_{\tau ml}(kn\boldsymbol{r}) \tag{3.7}$$

$$\boldsymbol{H}(\boldsymbol{r}) = \frac{1}{\mathrm{i}\eta_0\eta}\sum_{l=1}^{\infty}\sum_{m=-l}^{l}\sum_{\tau=1}^{2} b_{\tau ml}\boldsymbol{v}_{\bar{\tau}ml}(kn\boldsymbol{r}) \tag{3.8}$$

where $\boldsymbol{v}_{\tau ml}(kn\boldsymbol{r})$ are *regular* vector spherical waves, and $b_{\tau ml}$ the corresponding multipole coefficients. The regular vector spherical waves are defined by

$$\boldsymbol{v}_{1ml}(kn\boldsymbol{r}) = \mathrm{j}_l(knr)\boldsymbol{A}_{1ml}(\hat{\boldsymbol{r}}) \tag{3.9}$$

$$\boldsymbol{v}_{2ml}(kn\boldsymbol{r}) = \frac{(knr\mathrm{j}_l(knr))'}{knr}\boldsymbol{A}_{2ml}(\hat{\boldsymbol{r}}) + \sqrt{l(l+1)}\frac{\mathrm{j}_l(knr)}{knr}\boldsymbol{A}_{3ml}(\hat{\boldsymbol{r}}) \tag{3.10}$$

where $\mathrm{j}_l(x)$ are the *spherical Bessel* functions of order l, see *e.g.*, [2, 17, 19]. Here, $(\cdot)'$ denotes differentiation with respect to the argument knr.

Continuity of the tangential fields $\boldsymbol{E}_{\rm t}$ and $\boldsymbol{H}_{\rm t}$ in (3.1), (3.2), (3.7) and (3.8) for $r = a$ yields the following solution for the reflection coefficient defined by $a^{(1)}_{\tau ml} = \rho_{\tau l} a^{(2)}_{\tau ml}$:

$$\rho_{\tau l}(k) = \frac{-{\rm h}^{(2)}_l(ka)\left(kna{\rm j}_l(kna)\right)' + \nu_\tau(k){\rm j}_l(kna)\left(ka{\rm h}^{(2)}_l(ka)\right)'}{{\rm h}^{(1)}_l(ka)\left(kna{\rm j}_l(kna)\right)' - \nu_\tau(k){\rm j}_l(kna)\left(ka{\rm h}^{(1)}_l(ka)\right)'} \tag{3.11}$$

where $\nu_1 = \mu$ and $\nu_2 = \epsilon$, *cf.*, [27]. It is assumed that $\nu_\tau(k)$ can be represented by an asymptotic series at $k = 0$. It has been shown that $\rho_{\tau l} = {\rm e}^{-{\rm i}2ka}\rho^{\rm c}_{\tau l}$, where $\rho^{\rm c}_{\tau l}$ is the transform of a causal kernel, see [3]. It can be expected that $\rho^{\rm c}_{\tau l}(k) = o(k)$ as $k \hat{\to} \infty$, which means that $b_1 = 0$ for the Herglotz function corresponding to (2.5). A detailed study of the high-frequency asymptotics of the reflection coefficient has been performed in the Appendix, including *e.g.*, the Debye and Lorentz dispersion models, and it asserts this expectation for these material models. The low-frequency asymptotics is obtained from a Taylor series expansion yielding $\rho_{\tau l}(k) \sim 1 + {\rm i}2(ka)^{2l+1}c_{\tau l}$, or

$$-{\rm i}\log\rho_{\tau l}(k) \sim a^{(0)}_{2l+1}k^{2l+1} = 2(ka)^{2l+1}c_{\tau l}, \quad \text{as } k \to 0, \tag{3.12}$$

where

$$c_{\tau l} = \frac{2^{2l}(l+1)!l!}{(2l+1)!(2l)!}\frac{\nu_\tau(0) - 1}{l + 1 + \nu_\tau(0)l} \tag{3.13}$$

and $\nu_\tau(0)$ is the static response. The symbol $\sim$ denotes asymptotic equivalence and is defined in *e.g.*, [21]. Note that the low-frequency asymptotics of the TM (TE) wave reflection is independent of $\mu(0)$ ($\epsilon(0)$).

3.3 Optimization formulation

The following inequalities are obtained from (2.8) and (3.12), where $p = 1, 2 \ldots, l+1$, $a^{(0)}_{2l+1} = 2a^{2l+1}c_{\tau l}/{\rm c}_0^{2l+1}$ and $t_0 = 2a/{\rm c}_0$:

$$\begin{cases} \frac{G_1}{\pi}\log|\rho_0|^{-1} \le k_0 a + \sum_n {\rm Im}\left\{\left(\frac{k_0}{k_n}\right)\right\} \\ \frac{G_{l'+1}}{\pi}\log|\rho_0|^{-1} \le \frac{1}{2l'+1}\sum_n {\rm Im}\left\{\left(\frac{k_0}{k_n}\right)^{2l'+1}\right\}, \ l' = 1, 2, \ldots, l-1 \\ \frac{G_{l+1}}{\pi}\log|\rho_0|^{-1} \le c_{\tau l}(k_0 a)^{2l+1} + \frac{1}{2l+1}\sum_n {\rm Im}\left\{\left(\frac{k_0}{k_n}\right)^{2l+1}\right\} \end{cases} \tag{3.14}$$

where G_l is defined by (2.9), $k_0 = \omega_0/{\rm c}_0$ and $k_n = z_n/{\rm c}_0$. Note that exactly the same relations are obtained by using (2.14) and (2.18) and the substitution $s = -{\rm i}k{\rm c}_0$.

The narrowband model is now assumed, *i.e.*, let $G_p = B$ in (3.14). Note also that in general, $B \le G_p$. Hence, the assumption $G_p = B$ will simplify the analysis below without loss of generality. Let $k_0/k_n = \alpha_n - {\rm i}\beta_n = r_n{\rm e}^{-{\rm i}\theta_n}$, where $\beta_n > 0$, $r_n > 0$ and $0 < \theta_n < \pi$, and let $f = \frac{B}{\pi}\log|\rho_0|^{-1}$. The optimum solution to the inequalities in (3.14) can then be formulated as the solution to the following

constrained optimization problem:

$$\begin{cases} \max f \\ -\sum_n \operatorname{Im}\{\alpha_n - \mathrm{i}\beta_n\} + f \le k_0 a \\ -\frac{1}{2l'+1}\sum_n \operatorname{Im}\left\{(\alpha_n - \mathrm{i}\beta_n)^{2l'+1}\right\} + f \le 0,\ l' = 1, 2, \ldots, l-1 \\ -\frac{1}{2l+1}\sum_n \operatorname{Im}\left\{(\alpha_n - \mathrm{i}\beta_n)^{2l+1}\right\} + f \le c_{\tau l}(k_0 a)^{2l+1} \\ f \ge 0,\ \beta_n \ge 0 \end{cases} \tag{3.15}$$

where the variables are $(f, \{\alpha_n\}, \{\beta_n\})$. The second constraint above is ignored when $l = 1$. Note that $\beta_n = 0$ is equivalent to removing the corresponding zeros from the summations above.

The solution to the optimization problem (3.15) defines the Fano limit[1] for the reflection coefficient of the spherical waves, *i.e.*, $|\rho_0| \ge \rho_{\text{Fano}} = \mathrm{e}^{-\pi f/B}$. When $l = 1$, it is sufficient to use one single zero, and the solution can be uniquely obtained from a 2×2 non-linear system of equations, see [8]. However, when $l > 1$ the numerical solution to the non-convex optimization problem (3.15) will in general require a global optimization routine and an exhaustive search. Furhermore, for $l > 1$ the optimal number of zeros is not known. A straightforward relaxation of the narrowband Fano equations (3.15) is considered in Section 5 below.

4 Exact circuit analogy for the scattering of a homogeneous sphere

Recursive relationships for the spherical Hankel functions can be used to obtain an exact circuit analogy for the scattering of spherical waves as described below, *cf.*, also [6, 28].

The spherical Hankel functions $\mathrm{h}_l^{(j)}(z)$ satisfy the following initial relations:

$$\begin{cases} \dfrac{(z\mathrm{h}_0^{(1)}(z))'}{z} = \mathrm{i}\mathrm{h}_0^{(1)}(z) \\ -\mathrm{h}_1^{(1)}(z) = \mathrm{i}\mathrm{h}_0^{(1)}(z)\left(1 - \dfrac{1}{\mathrm{i}z}\right), \end{cases} \quad \begin{cases} \dfrac{(z\mathrm{h}_0^{(2)}(z))'}{z} = -\mathrm{i}\mathrm{h}_0^{(2)}(z) \\ -\mathrm{h}_1^{(2)}(z) = -\mathrm{i}\mathrm{h}_0^{(2)}(z)\left(1 + \dfrac{1}{\mathrm{i}z}\right), \end{cases} \tag{4.1}$$

and the recursive relations

$$\begin{cases} \dfrac{(z\mathrm{h}_l^{(j)}(z))'}{z\mathrm{i}^l} = \dfrac{\mathrm{h}_{l-1}^{(j)}(z)}{\mathrm{i}^l} + \dfrac{l}{-\mathrm{i}z}\dfrac{-\mathrm{h}_l^{(j)}(z)}{\mathrm{i}^{l+1}} \\ \dfrac{\mathrm{h}_{l+1}^{(j)}(z)}{\mathrm{i}^{l+2}} = \dfrac{\mathrm{h}_{l-1}^{(j)}(z)}{\mathrm{i}^l} + \dfrac{2l+1}{-\mathrm{i}z}\dfrac{-\mathrm{h}_l^{(j)}(z)}{\mathrm{i}^{l+1}} \end{cases} \tag{4.2}$$

for $j = 1, 2$ and $l = 1, 2, \ldots$, see *e.g.*, [2, 17, 19].

[1] The term Fano limit is used here even though the scattering problem is different from the matching problem. This is motivated by the equivalence of these problems as discussed in this paper.

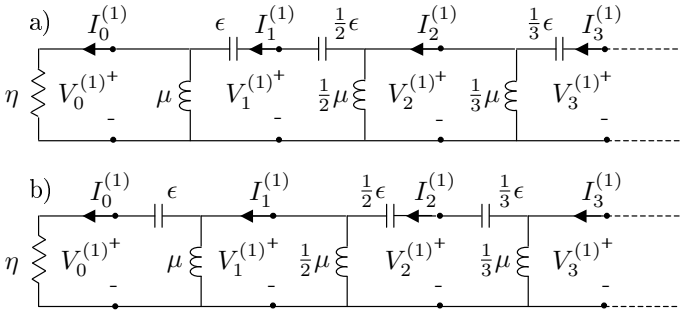

Figure 4: The two dual electric circuits with termination representing spherical Hankel functions of the first kind $\mathrm{h}_l^{(1)}(z)$, *i.e.*, outgoing waves outside a sphere of radius a.

There are two possible dual circuits associated with the recursions in (4.1) and (4.2), *cf.*, Figure 4. For circuit a), define

$$\frac{(z\mathrm{h}_l^{(j)}(z))'}{z\mathrm{i}^l} = \begin{cases} \eta I_l^{(j)}(z) & l = 0, 2, 4, \ldots \\ -V_l^{(j)}(z) & l = 1, 3, 5, \ldots \end{cases} \tag{4.3}$$

and

$$-\frac{\mathrm{h}_l^{(j)}(z)}{\mathrm{i}^{l+1}} = \begin{cases} V_l^{(j)}(z) & l = 0, 2, 4, \ldots \\ -\eta I_l^{(j)}(z) & l = 1, 3, 5, \ldots \end{cases} \tag{4.4}$$

where $V_l(z)$ and $I_l(z)$ represent voltages and currents, respectively.

Let $z = \kappa n$, where $\kappa = ka$ and $n = (\mu\epsilon)^{1/2}$. By introducing the normalized Laplace variable $S = -\mathrm{i}\kappa = sa/\mathrm{c}_0$ and employing the definitions in (4.3) and (4.4), the following initial relations for $V_l(z)$ and $I_l(z)$ corresponding to (4.1) are obtained:

$$\begin{cases} \eta I_0^{(1)}(z) = V_0^{(1)}(z) \\ I_1^{(1)}(z) = I_0^{(1)}(z) + V_0^{(1)}(z)\dfrac{1}{S\mu}, \end{cases} \quad \begin{cases} \eta I_0^{(2)}(z) = -V_0^{(2)}(z) \\ I_1^{(2)}(z) = I_0^{(2)}(z) + V_0^{(2)}(z)\dfrac{1}{S\mu}, \end{cases} \tag{4.5}$$

and the recursive relations corresponding to (4.2) are given by

$$\begin{cases} V_l^{(j)}(z) = V_{l-1}^{(j)}(z) + \dfrac{1}{S\epsilon\frac{1}{l}} I_l^{(j)}(z) & l = 1, 3, 5, \ldots \\ I_l^{(j)}(z) = I_{l-1}^{(j)}(z) + \dfrac{1}{S\mu\frac{1}{l}} V_l^{(j)}(z) & l = 2, 4, 6, \ldots \\ V_{l+1}^{(j)}(z) = V_{l-1}^{(j)}(z) + \dfrac{1}{S\epsilon\frac{1}{2l+1}} I_l^{(j)}(z) & l = 1, 3, 5, \ldots \\ I_{l+1}^{(j)}(z) = I_{l-1}^{(j)}(z) + \dfrac{1}{S\mu\frac{1}{2l+1}} V_l^{(j)}(z) & l = 2, 4, 6, \ldots \end{cases} \tag{4.6}$$

where $j = 1, 2$. The dual circuit b) is obtained by interchanging $V_l \leftrightarrow \eta I_l$, or equivalently, by simultaneously interchanging $V_l \leftrightarrow I_l$ and $\mu \leftrightarrow \epsilon$.

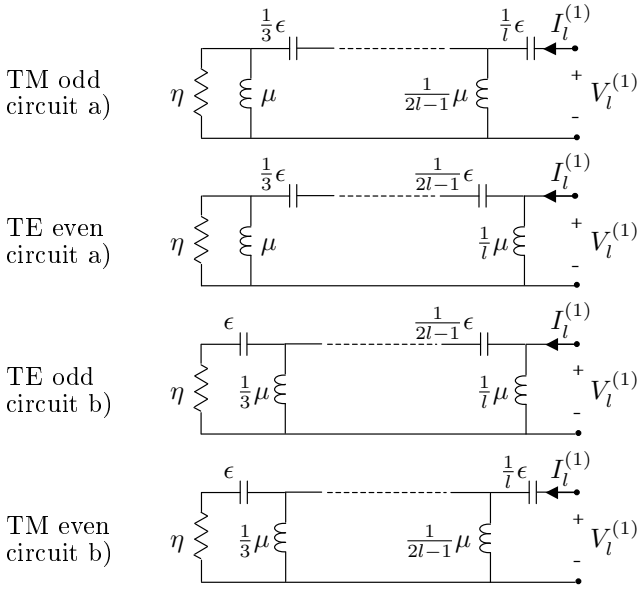

Figure 5: Electric circuit analogy for TM and TE waves of odd and even order, corresponding to spherical Hankel functions of the first kind $\mathrm{h}_l^{(1)}(z)$, *i.e.*, outgoing waves outside a sphere of radius a.

4.1 Exterior of the sphere

Consider now the free space exterior of the sphere where $r \geq a$ and $z = \kappa = ka$ ($\mu = \epsilon = \eta = n = 1$). In Figure 4 is shown the two dual electric circuits with termination representing spherical Hankel functions of the first kind $\mathrm{h}_l^{(1)}(z)$, corresponding to outgoing vector spherical waves. There are four different circuits representing the TM and TE waves of odd and even order, as depicted in Figure 5. In Figure 6 is shown the excitation with a Hankel function generator for the two dual electric circuits representing spherical Hankel functions of the second kind $\mathrm{h}_l^{(2)}(z)$, corresponding to incoming vector spherical waves.

From the field definition (3.1) and (3.2) and the circuit (and its dual) definition (4.3) and (4.4), the tangential fields $\boldsymbol{E}_{\mathrm{t},ml}$ and $\boldsymbol{H}_{\mathrm{t},ml}$ (spherical wave indices m, l for $\tau = 1, 2$) outside the sphere are given by

$$\begin{cases} \boldsymbol{E}_{\mathrm{t},ml} = \mp \mathrm{i}^{l+1} \boldsymbol{A}_{1ml} \left(a_{1ml}^{(1)} V_l^{(1)} + a_{1ml}^{(2)} V_l^{(2)} \right) \pm \mathrm{i}^{l} \boldsymbol{A}_{2ml} \left(a_{2ml}^{(1)} V_l^{(1)} + a_{2ml}^{(2)} V_l^{(2)} \right) \\ \eta_0 \boldsymbol{H}_{\mathrm{t},ml} = \mp \mathrm{i}^{l} \boldsymbol{A}_{1ml} \left(a_{2ml}^{(1)} I_l^{(1)} + a_{2ml}^{(2)} I_l^{(2)} \right) \mp \mathrm{i}^{l+1} \boldsymbol{A}_{2ml} \left(a_{1ml}^{(1)} I_l^{(1)} + a_{1ml}^{(2)} I_l^{(2)} \right) \end{cases} \tag{4.7}$$

where the arguments $\boldsymbol{r}$, $\hat{\boldsymbol{r}}$ and $z = \kappa$ have been suppressed for simplicity, and the upper and lower signs refer to even and odd orders, respectively. The normalized

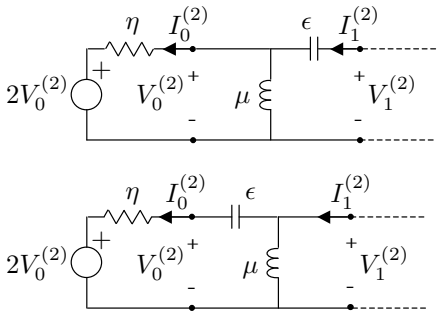

Figure 6: Excitation with a Hankel function generator for the two dual electric circuits representing spherical Hankel functions of the second kind $\mathrm{h}_l^{(2)}(z)$, *i.e.*, incoming waves outside a sphere of radius a.

TE and TM wave impedances $Z_{\tau l}^{(j)}(z)$ are given by

$$\begin{cases} Z_{1l}^{(j)}(z) = \dfrac{V_l^{(j)}(z)}{I_l^{(j)}(z)} = \mathrm{i}\eta \dfrac{z\mathrm{h}_l^{(j)}(z)}{(z\mathrm{h}_l^{(j)}(z))'} \\ Z_{2l}^{(j)}(z) = \dfrac{V_l^{(j)}(z)}{I_l^{(j)}(z)} = -\mathrm{i}\eta \dfrac{(z\mathrm{h}_l^{(j)}(z))'}{z\mathrm{h}_l^{(j)}(z)} \end{cases} \tag{4.8}$$

where $j = 1, 2$ correspond to the outgoing and incoming waves, respectively.

4.2 Interior of the sphere

Next, consider the interior of the sphere where $r \leq a$, $z = \kappa n = kan$ and $n = (\mu\epsilon)^{1/2}$. In Figure 7 is shown the two dual electric circuits with termination representing spherical Hankel functions of the second kind $\mathrm{h}_l^{(2)}(z)$, corresponding to incoming vector spherical waves. The circuit definitions (4.3) and (4.4) and recursions (4.5) and (4.6) are the same, but the circuit interpretation is different with an opposite direction for $I_l^{(j)}(z)$ and a sign change of μ and ϵ. These changes correspond precisely to the symmetry of the incoming and outgoing wave impedances

$$Z_{\tau l}^{(2)}(z) = -Z_{\tau l}^{(1)}(-z) \tag{4.9}$$

defined in (4.8). The four different circuits representing odd and even TM and TE waves in Figure 5 are changed accordingly. In Figure 8 is shown the excitation with a Hankel function generator for the two dual electric circuits representing spherical Hankel functions of the first kind $\mathrm{h}_l^{(1)}(z)$, corresponding to outgoing vector spherical waves. The circuit elements with impedances $S\mu$ and $1/S\epsilon$ are regarded as "generalized" inductors and capacitors in case the material is dispersive. However, these circuit elements behave asymptotically as "true" inductors and capacitors in the low-frequency limit. Hence, $S\mu \sim S\mu(0)$ and $1/S\epsilon \sim 1/S\epsilon(0)$ when $S \to 0$.

From the field definition (3.7) and (3.8) and the circuit (and its dual) definition (4.3) and (4.4), the tangential fields $\boldsymbol{E}_{\mathrm{t},ml}$ and $\boldsymbol{H}_{\mathrm{t},ml}$ (spherical wave indices m, l for

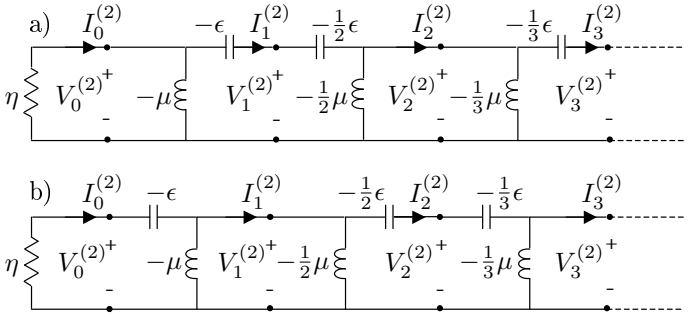

Figure 7: The two dual electric circuits with termination representing spherical Hankel functions of the second kind $\mathrm{h}_l^{(2)}(z)$, *i.e.*, incoming waves inside a sphere of radius a.

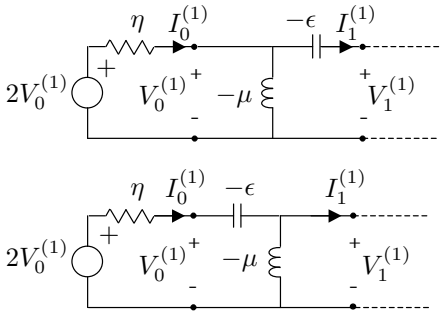

Figure 8: Excitation with a Hankel function generator for the two dual electric circuits representing spherical Hankel functions of the first kind $\mathrm{h}_l^{(1)}(z)$, *i.e.*, outgoing waves inside a sphere of radius a.

$\tau = 1, 2$) inside the sphere are given by

$$\begin{cases} \boldsymbol{E}_{\mathrm{t},ml} = \mp \mathrm{i}^{l+1} \boldsymbol{A}_{1ml} \dfrac{b_{1ml}}{2} \left(V_l^{(1)} + V_l^{(2)} \right) \pm \mathrm{i}^{l} \boldsymbol{A}_{2ml} \dfrac{b_{2ml}}{2} \left(V_l^{(1)} + V_l^{(2)} \right) \\ \eta_0 \boldsymbol{H}_{\mathrm{t},ml} = \mp \mathrm{i}^{l} \boldsymbol{A}_{1ml} \dfrac{b_{2ml}}{2} \left(I_l^{(1)} + I_l^{(2)} \right) \mp \mathrm{i}^{l+1} \boldsymbol{A}_{2ml} \dfrac{b_{1ml}}{2} \left(I_l^{(1)} + I_l^{(2)} \right) \end{cases} \tag{4.10}$$

where the arguments $\boldsymbol{r}$, $\hat{\boldsymbol{r}}$ and $z = \kappa n$ have been suppressed for simplicity, and the upper and lower signs refer to even and odd orders, respectively. The normalized TE and TM wave impedances $Z_{\tau l}^{(j)}$ are given by (4.8) with $z = \kappa n$.

4.3 Exact circuit analogy for the scattering

The scattering problem in Section 3 can now be interpreted by using an exact (equivalent) circuit analogy where the exterior and the interior tangential fields (4.7) and (4.10) are perfectly matched as depicted in Figure 9. An independent exterior generator is used to generate the incoming waves, and a dependent interior generator is used to create the outgoing waves and hence the Bessel functions (obtained as the superposition of the two kinds of Hankel functions) within the sphere, see also [28]. The dependent interior generator and its internal resistance correspond to a

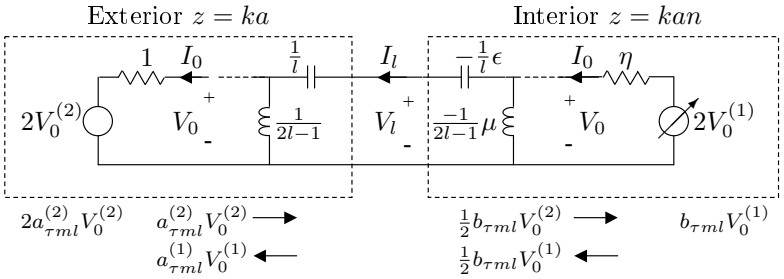

Figure 9: Scattering model with Hankel function generators and matching. The interior generator is dependent, creating Bessel functions corresponding to standing waves within the sphere. The circuits are drawn for TM_l waves. The TE_l waves are similar.

reflection coefficient

$$\mathit{\Gamma}(\kappa n) = \frac{V_0^{(1)}(\kappa n)}{V_0^{(2)}(\kappa n)} = (-1)^{\tau+l}\mathrm{e}^{\mathrm{i}2\kappa n}. \tag{4.11}$$

Note that in the equivalent circuit analogy depicted in Figure 9, the voltage and current constituents $V_l^{(j)}$ and $I_l^{(j)}$ with $j = 1, 2$, correspond to a wave splitting with respect to the generator or termination impedance η, *cf.*, also Figures 6 and 8.

The circuit problem, and hence the scattering problem, has a unique solution through the scattering (S-matrix) relations

$$\begin{cases} a_{\tau ml}^{(1)}V_0^{(1)}(\kappa) &= \rho_{1,\tau l}^{\mathrm{c}} a_{\tau ml}^{(2)}V_0^{(2)}(\kappa) + \varrho_{2,\tau l}^{\mathrm{c}} \frac{1}{2} b_{\tau ml}V_0^{(1)}(\kappa n) \\ \frac{1}{2}b_{\tau ml}V_0^{(2)}(\kappa n) &= \varrho_{1,\tau l}^{\mathrm{c}} a_{\tau ml}^{(2)}V_0^{(2)}(\kappa) + \rho_{2,\tau l}^{\mathrm{c}} \frac{1}{2} b_{\tau ml}V_0^{(1)}(\kappa n) \end{cases} \tag{4.12}$$

where $(\rho_{1,\tau l}^{\mathrm{c}}, \varrho_{1,\tau l}^{\mathrm{c}}, \rho_{2,\tau l}^{\mathrm{c}}, \varrho_{2,\tau l}^{\mathrm{c}})$ are the scattering parameters of the equivalent circuit representing the exterior as well as the interior of the sphere. Here, $a_{\tau ml}^{(2)}$ is the amplitude of the incoming wave and (4.12) can be solved for the amplitudes of the outgoing wave $a_{\tau ml}^{(1)}$ and the Bessel function (standing wave) amplitude $b_{\tau ml}$. The overall reflection coefficient $\rho_{\tau l}^{\mathrm{c}}$ for the equivalent circuit is given by

$$\rho_{\tau l}^{\mathrm{c}} = \frac{V_0^{(1)}(\kappa)a_{\tau ml}^{(1)}}{V_0^{(2)}(\kappa)a_{\tau ml}^{(2)}} = (-1)^{\tau+l}\mathrm{e}^{\mathrm{i}2\kappa}\rho_{\tau l} \tag{4.13}$$

where $\rho_{\tau l}$ is the reflection coefficent given by (3.11).

Note that the presence of the negative circuit elements in Figure 9 is consistent with the fact that the wave impedance $Z_{\tau l}^{(2)}$ for incoming waves at $r = a$ is anticausal, *cf.*, (4.8) and (4.9). However, note also that the overall equivalent circuit is causal due to the delay factor in (4.13) above.

The low-frequency asymptotics of the function $-\mathrm{i}\log\left\{(-1)^{\tau+l}\rho_{\tau l}^{\mathrm{c}}\right\}$ corresponding to (4.13) is given by

$$-\mathrm{i}\log\left\{(-1)^{\tau+l}\rho_{\tau l}^{\mathrm{c}}\right\} \sim 2\kappa + 2\kappa^{2l+1}c_{\tau l} \tag{4.14}$$

where $c_{\tau l}$ is given by (3.13). The high-frequency asymptotics is

$$-\mathrm{i}\log\left\{(-1)^{\tau+l}\rho^{\mathrm{c}}_{\tau l}(\kappa)\right\} = -\mathrm{i}\log\left\{\mathrm{e}^{\mathrm{i}2\kappa}\rho_{\tau l}(\kappa)\right\} = \kappa b_1 \mathrm{c}_0/a + o(\kappa) \tag{4.15}$$

as $\kappa \to \infty$, where $b_1 \geq 0$. Furthermore, it is expected that $b_1 = 0$ for many material models as discussed in Section 3.2.

Note that the circuit elements corresponding to the interior in Figure 9 behave as $S\mu \sim S\mu(0)$ and $1/S\epsilon \sim 1/S\epsilon(0)$ when $S = -\mathrm{i}\kappa \to 0$. Note also that the low-frequency asymptotics of the TM (TE) reflection coefficient $\rho_{\tau l}$, *i.e.*, the coefficient $c_{\tau l}$, is independent of $\mu(0)$ ($\epsilon(0)$). Hence, when considering the high-contrast limit of the low-frequency asymptotics (4.14) in the TM (TE) case, the limit $\epsilon(0) \to \infty$ ($\mu(0) \to \infty$) may be carried out using $\epsilon(0) = \mu(0) \to \infty$. In this limit, the circuit elements with impedances $S\mu(0)$ and $1/S\epsilon(0)$ behave as open and short circuits, respectively. Further, the low-frequency asymptotics of (4.11) is $\Gamma(\kappa n) \sim (-1)^{\tau+l}$ as $\kappa \to 0$. Hence, the high-contrast limit of the low-frequency asymptotics in (4.14) may be obtained equivalently by using the exterior circuit with open or short termination as depicted in Figure 10. This means that the low-frequency asymptotics of $\rho_{1,\tau l}$ according to the conjecture (2.17) and (2.18) is identical to (4.14) with $-\mathrm{i}\kappa = s\frac{a}{\mathrm{c}_0}$, and hence

$$-\log\left\{(-1)^{\tau+l}\rho_{1,\tau l}\right\} \sim 2\frac{a}{\mathrm{c}_0}s + 2(-1)^l(\frac{a}{\mathrm{c}_0})^{2l+1}c_{\tau l}s^{2l+1} \tag{4.16}$$

where

$$c_{\tau l} = \frac{2^{2l}(l+1)!(l-1)!}{(2l+1)!(2l)!} \tag{4.17}$$

is the high-contrast limit of (3.13) when $\nu_\tau(0) \to \infty$. Note that the exterior circuit has a transmission zero of order $l+1$ at $S = 0$ and the term $2\kappa^{2l+1}c_{\tau l}$ of the reflection coefficient $\rho_{1,\tau l}$ is therefore invariant to whether the circuit is terminated with a short, open or match, *cf.*, (2.15). Note also the interesting distinguishing feature that the integral identity (2.14) contains no causality term t_0 as in (2.7), instead this term $t_0 = 2a/c_0$ appears in the low-frequency asymptotics of $-\log\{\rho_{1,\tau l}\}$ as $A_1^{(0)}$ in (2.17) and (4.16).

In conclusion, the optimal Fano matching problem for the exterior circuit as described in Section 2.3 is equivalent to the problem of determining the optimal limitations for scattering of spherical waves in the high-contrast limit as described in Section 3.3. An exact expression for the low-frequency asymptotics of $-\log\{\rho_{1,\tau l}\}$ is given by (4.16) and (4.17). The exact expression agree perfectly with the numerical results given in [29].

5 Numerical example: relaxation of the Fano equations

As a numerical example, a relaxation of the narrowband Fano equations (3.15) is considered below. To solve (3.15) for $l \geq 2$, one has to resort to global optimization

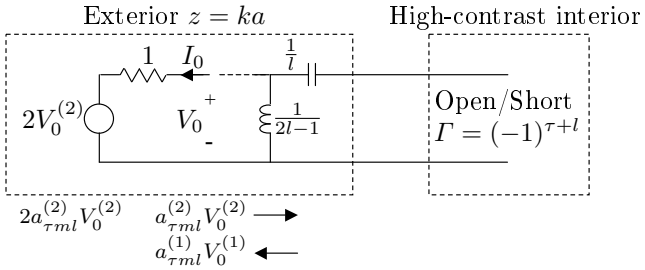

Figure 10: Interpretation of the scattering model in the high-contrast limit, $\epsilon(0) = \mu(0) \to \infty$. The exterior circuit is drawn for TM_l waves. The TE_l waves are similar.

and computationally expensive numerical experiments. Hence, a straightforward relaxation yielding an upper bound on the objective function f may be useful.

In order to relax the constraints in (3.15), consider the minimization of the expression $-\frac{1}{2l+1}\sum_n \mathrm{Im}\left\{(\alpha_n - \mathrm{i}\beta_n)^{2l+1}\right\} = \frac{1}{2l+1}\sum_n \beta_n^{2l+1}\frac{\sin(\theta_n(2l+1))}{\sin^{2l+1}\theta_n}$ when β_n is fixed. This implies the stationarity condition $\frac{\partial}{\partial \alpha_n}\mathrm{Im}\left\{(\alpha_n - \mathrm{i}\beta_n)^{2l+1}\right\} = 0$ yielding the solutions, $(r_n, \theta_n) = \left(\frac{\beta_n}{\sin(m\frac{\pi}{2l})}, m\frac{\pi}{2l}\right)$ where $m = 1, \ldots, 2l-1$. Hence, by choosing

$$-d_l = \min_{1 \le m \le 2l-1} \frac{1}{2l+1}\frac{\sin(m\frac{\pi}{2l}(2l+1))}{\sin^{2l+1}(m\frac{\pi}{2l})} \tag{5.1}$$

where $d_l > 0$, and by employing $\left(\sum_{n=1}^N \beta_n\right)^{2l+1} \ge \sum_{n=1}^N \beta_n^{2l+1}$, a relaxation of (3.15) valid for all N is given by

$$\begin{cases} \max f \\ \beta + f \le k_0 a \\ -d_{l'}\beta^{2l'+1} + f \le 0, \ l' = 1, \ldots, l-1 \\ -d_l\beta^{2l+1} + f \le c_{\tau l}(k_0 a)^{2l+1} \\ f \ge 0, \ \beta \ge 0 \end{cases} \tag{5.2}$$

where there are two variables (f, β). The solution to (5.2) yields an upper bound for the corresponding Fano limit in the variable f. Hence, $|\rho_0| \ge \rho_{\text{Fano}} \ge \mathrm{e}^{-\pi f/B}$. When $l = 1$, the relaxation becomes tight and the solution to (5.2) is identical to the Fano limit ($l = 1 \Rightarrow \theta_n = \pi/2$). Furthermore, for $l = 1$ there is a transition point where the second constraint becomes inactive and hence $f = k_0 a$ for $k_0 a \ge \sqrt{1/c_{\tau 1}}$. To solve (5.2) for $l \ge 2$, it is noted that the first (linear) constraint is always active. Since the polynomial constraints are monotonic in β for $\beta \ge 0$, the optimum solution is found as the minimum of f over the l constraint subsets corresponding to a 2×2 non-linear system of equations containing the first linear constraint $\beta + f = k_0 a$. Note that each such constraint subset has a unique solution for $\beta \ge 0$. The asymptotic solution to (5.2) when $k_0 a \to 0$ is given by

$$f = (d_l + c_{\tau l})(k_0 a)^{2l+1} + \mathcal{O}\left((k_0 a)^{2l+3}\right). \tag{5.3}$$

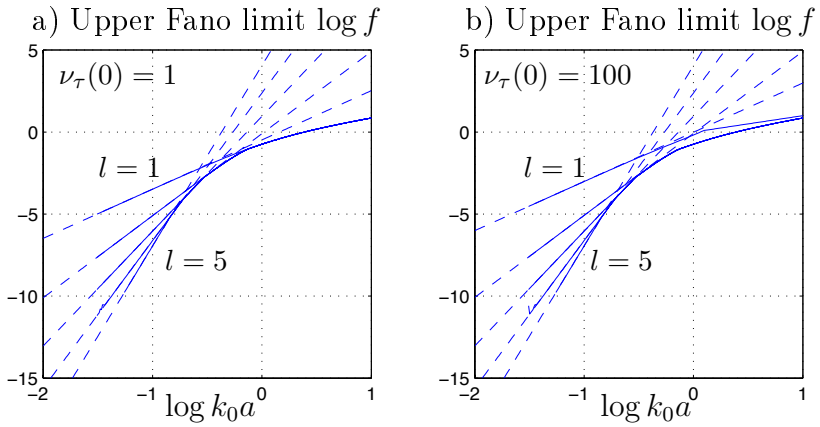

Figure 11: Upper Fano limit f as a function of k_0a for $l = 1, 2, \ldots, 5$. Graphs a and b show $\log f$ for $\nu_\tau(0) = 1$ and $\nu_\tau(0) = 100$, respectively. The dashed lines show the asymptotic upper bounds $(d_l + c_{\tau l})(k_0a)^{2l+1}$ in the narrowband approximation where $G_l = B$.

For $l \geq 2$, the asymptotic solution to (5.2) when $k_0a \to \infty$ is governed by the lowest index $l' = 1$ and is hence given by the solution to the first two constraints, *i.e.*, the real valued root of $f = (k_0a - f)^3/3$. In Figure 11 is shown the upper Fano limit f as a function of k_0a for $l = 1, 2, \ldots, 5$ and $\nu_\tau(0) = 1, 100$, respectively.

6 Summary

Optimal limitations for the scattering of vector spherical waves is considered where the geometry of the object is known but the temporal dispersion is unknown. Using integral relations similar to the derivation of Fano's broadband matching bounds, the optimal scattering limitations are determined by the static response as well as the high-frequency asymptotics of the reflection coefficient. Using an exact circuit analogy for the scattering of spherical waves, it is shown how the problem of determining the optimal scattering bounds for a homogeneous sphere in its high-contrast limit becomes identical to the closely related, and yet very different problem of finding the broadband tuning limits of the spherical waves. Furthermore, the scattering view of the matching problem yields explicitly the necessary low frequency asymptotics of the reflection coefficient that is used with Fano's broadband matching bounds for spherical waves, something that appears to be non-trivial to derive from the classical network point of view.

As with the Fano approach, the integral relations yield a non-convex global optimization problem which in general is quite difficult to handle. As a numerical example, a relaxation of the Fano equations is considered which is easily solved and which is especially useful in the regime of Rayleigh scattering.

Appendix A High-frequency asymptotics of scattering coefficients

To find the dominant behavior of the reflection coefficients $\rho_{\tau l}$ in (3.11) for high frequencies, the asymptotic behavior of the spherical Bessel and Hankel functions are needed. For large arguments the spherical Hankel functions behave as [1]

$$\begin{cases} \mathrm{h}_l^{(1)}(z) = (-\mathrm{i})^{l+1}\dfrac{\mathrm{e}^{\mathrm{i}z}}{z}\left(1+\mathrm{i}\dfrac{a_l}{z}-\dfrac{b_l}{z^2}+\mathcal{O}(z^{-3})\right) \\ \mathrm{h}_l^{(2)}(z) = \mathrm{i}^{l+1}\dfrac{\mathrm{e}^{-\mathrm{i}z}}{z}\left(1-\mathrm{i}\dfrac{a_l}{z}-\dfrac{b_l}{z^2}+\mathcal{O}(z^{-3})\right) \\ \left(z\mathrm{h}_l^{(1)}(z)\right)' = (-\mathrm{i})^{l+1}\mathrm{e}^{\mathrm{i}z}\left(\mathrm{i}-\dfrac{a_l}{z}-\mathrm{i}\dfrac{a_l+b_l}{z^2}+\mathcal{O}(z^{-3})\right) \\ \left(z\mathrm{h}_l^{(2)}(z)\right)' = \mathrm{i}^{l+1}\mathrm{e}^{-\mathrm{i}z}\left(-\mathrm{i}-\dfrac{a_l}{z}+\mathrm{i}\dfrac{a_l+b_l}{z^2}+\mathcal{O}(z^{-3})\right) \end{cases} \tag{A.1}$$

as $z \to \infty$, where z is complex valued, $a_l = (l+1)l/2$ and $b_l = (l+2)(l+1)l(l-1)/8$, and the big ordo notation $\mathcal{O}$ is defied as in [21]. Moreover, as $z \to \infty$ the spherical Bessel functions behave as [1]

$$\begin{cases} \mathrm{j}_l(z) = \dfrac{1}{z}\left\{\left(1-\dfrac{b_l}{z^2}+\mathcal{O}(z^{-4})\right)\sin\left(z-\dfrac{l\pi}{2}\right)+\left(\dfrac{a_l}{z}+\mathcal{O}(z^{-3})\right)\cos\left(z-\dfrac{l\pi}{2}\right)\right\} \\ (z\mathrm{j}_l(z))' = \left(1-\dfrac{a_l+b_l}{z^2}+\mathcal{O}(z^{-4})\right)\cos\left(z-\dfrac{l\pi}{2}\right)-\left(\dfrac{a_l}{z}+\mathcal{O}(z^{-3})\right)\sin\left(z-\dfrac{l\pi}{2}\right). \end{cases} \tag{A.2}$$

To find the high-frequency behavior of (3.11), special care must be taken to separate the exponential behavior of ka and the algebraic behavior of ka. To this end, expand the material parameters as a power series at infinity, *i.e.*,

$$\begin{cases} \nu_\tau = \alpha_0 + \dfrac{\mathrm{i}\alpha_1}{\kappa} + \dfrac{\alpha_2}{\kappa^2} + \mathcal{O}\left(\kappa^{-3}\right) \\ \kappa n = \kappa\left(\beta_0 + \frac{\mathrm{i}\beta_1}{\kappa} + \frac{\beta_2}{\kappa^2} + \frac{\mathrm{i}\beta_3}{\kappa^3} + \mathcal{O}\left(\kappa^{-4}\right)\right) = \beta_0\kappa + \mathrm{i}\beta_1 + \frac{\beta_2}{\kappa} + \frac{\mathrm{i}\beta_3}{\kappa^2} + \mathcal{O}\left(\kappa^{-3}\right) \end{cases} \tag{A.3}$$

where $\kappa = ka$, $\kappa \to \infty$, and where $\alpha_0, \alpha_1, \alpha_2 \in \mathbb{R}$ and $\beta_0, \beta_1, \beta_2, \beta_3 \in \mathbb{R}$. The last power series includes the Debye and the Lorentz dispersion models [19]. In particular, the Debye dispersion model (with real valued and positive parameters ϵ_∞, ϵ_s and τ) is given by

$$\epsilon(\kappa) = \epsilon_\infty + \frac{\epsilon_\mathrm{s}-\epsilon_\infty}{1-\mathrm{i}\kappa\tau} = \epsilon_\infty + \mathrm{i}\frac{\epsilon_\mathrm{s}-\epsilon_\infty}{\kappa\tau} + \frac{\epsilon_\mathrm{s}-\epsilon_\infty}{\kappa^2\tau^2} + \mathcal{O}(\kappa^{-3}) \tag{A.4}$$

and the Lorentz dispersion model (with real valued and positive parameters ϵ_∞, κ_p, κ_0 and ς)

$$\epsilon(\kappa) = \epsilon_\infty - \frac{\kappa_\mathrm{p}^2}{\kappa^2-\kappa_0^2+\mathrm{i}\kappa\varsigma} = \epsilon_\infty - \frac{\kappa_\mathrm{p}^2}{\kappa^2} + \mathrm{i}\frac{\kappa_\mathrm{p}^2\varsigma}{\kappa^3} + \mathcal{O}(\kappa^{-4}) \tag{A.5}$$

as $\kappa \to \infty$, which also motivates the assumption of real-valued coefficients in the expansion. If α_1 or β_1 is non-zero, then ν_τ corresponds effectively to a Debye model or a conductivity model. If both are zero, the model is of Lorentz' type. These expansions imply

$$\left\{\begin{array}{rcl} \sin\left(\kappa n - \dfrac{l\pi}{2}\right) &=& \sin\left(\beta_0\kappa - \frac{l\pi}{2} + \mathrm{i}\beta_1 + \frac{\beta_2}{\kappa} + \frac{\mathrm{i}\beta_3}{\kappa^2} + \mathcal{O}(\kappa^{-3})\right) \\ &=& A\sin\left(\beta_0\kappa - \frac{l\pi}{2} + \mathrm{i}\beta_1\right) + B\cos\left(\beta_0\kappa - \frac{l\pi}{2} + \mathrm{i}\beta_1\right) \\ \cos\left(\kappa n - \dfrac{l\pi}{2}\right) &=& \cos\left(\beta_0\kappa - \frac{l\pi}{2} + \mathrm{i}\beta_1 + \frac{\beta_2}{\kappa} + \frac{\mathrm{i}\beta_3}{\kappa^2} + \mathcal{O}(\kappa^{-3})\right) \\ &=& A\cos\left(\beta_0\kappa - \frac{l\pi}{2} + \mathrm{i}\beta_1\right) - B\sin\left(\beta_0\kappa - \frac{l\pi}{2} + \mathrm{i}\beta_1\right) \end{array}\right. \tag{A.6}$$

where

$$\left\{\begin{array}{l} A = \cos\left(\frac{\beta_2}{\kappa} + \frac{\mathrm{i}\beta_3}{\kappa^2} + \mathcal{O}(\kappa^{-3})\right) = 1 - \frac{\beta_2^2}{2\kappa^2} + \mathcal{O}(\kappa^{-3}) \\ B = \sin\left(\frac{\beta_2}{\kappa} + \frac{\mathrm{i}\beta_3}{\kappa^2} + \mathcal{O}(\kappa^{-3})\right) = \frac{\beta_2}{\kappa} + \frac{\mathrm{i}\beta_3}{\kappa^2} + \mathcal{O}(\kappa^{-3}). \end{array}\right. \tag{A.7}$$

The quantities $\rho_{\tau l}$ are now studied. Introduce the appropriate numerator N_l and denominator D_l such that

$$\rho_{\tau l} = -\mathrm{e}^{-2\mathrm{i}\kappa}(-1)^{l+1}\rho^{\mathrm{c}}_{\tau l} = \mathrm{e}^{-2\mathrm{i}(\kappa - l\pi/2)}\rho^{\mathrm{c}}_{\tau l} = \mathrm{e}^{-2\mathrm{i}(\kappa - l\pi/2)}\frac{N_l}{D_l} \tag{A.8}$$

where the numerator N_l is

$$\begin{aligned} N_l = \left(1 - \mathrm{i}\frac{a_l}{\kappa} - \frac{b_l}{\kappa^2} + \mathcal{O}(\kappa^{-3})\right)(\kappa n \mathrm{j}_l(\kappa n))' \\ - \nu_\tau\kappa\left(-\mathrm{i} - \frac{a_l}{\kappa} + \mathrm{i}\frac{a_l + b_l}{\kappa^2} + \mathcal{O}(\kappa^{-3})\right)\mathrm{j}_l(\kappa n) \end{aligned} \tag{A.9}$$

and the denominator is

$$\begin{aligned} D_l = \left(1 + \mathrm{i}\frac{a_l}{\kappa} - \frac{b_l}{\kappa^2} + \mathcal{O}(\kappa^{-3})\right)(\kappa n \mathrm{j}_l(\kappa n))' \\ - \nu_\tau\kappa\left(\mathrm{i} - \frac{a_l}{\kappa} - \mathrm{i}\frac{a_l + b_l}{\kappa^2} + \mathcal{O}(\kappa^{-3})\right)\mathrm{j}_l(\kappa n). \end{aligned} \tag{A.10}$$

Moreover, as $ka = \kappa \to \infty$ the power series expansions defined above yield after some algebra

$$\left\{\begin{array}{rl} N_l &= \left(1 + \mathrm{i}\frac{\alpha_0(a_l + \beta_0\beta_2) - a_l\beta_0^2}{\beta_0^2\kappa} + \mathcal{O}(\kappa^{-2})\right)\cos(\beta_0\kappa - \frac{l\pi}{2} + \mathrm{i}\beta_1) \\ &\quad + \mathrm{i}\left(\frac{\alpha_0}{\beta_0} - \mathrm{i}\frac{(\alpha_0 - 1)a_l\beta_0 + \alpha_0\beta_1 - \beta_0(\alpha_1 + \beta_0\beta_2)}{\beta_0^2\kappa} + \mathcal{O}(\kappa^{-2})\right)\sin(\beta_0\kappa - \frac{l\pi}{2} + \mathrm{i}\beta_1) \\ D_l &= \left(1 - \mathrm{i}\frac{\alpha_0(a_l + \beta_0\beta_2) - a_l\beta_0^2}{\beta_0^2\kappa} + \mathcal{O}(\kappa^{-2})\right)\cos(\beta_0\kappa - \frac{l\pi}{2} + \mathrm{i}\beta_1) \\ &\quad - \mathrm{i}\left(\frac{\alpha_0}{\beta_0} + \mathrm{i}\frac{(\alpha_0 - 1)a_l\beta_0 - \alpha_0\beta_1 + \beta_0(\alpha_1 - \beta_0\beta_2)}{\beta_0^2\kappa} + \mathcal{O}(\kappa^{-2})\right)\sin(\beta_0\kappa - \frac{l\pi}{2} + \mathrm{i}\beta_1). \end{array}\right. \tag{A.11}$$

For simplicity, assume that there is no optical response *i.e.*, $\alpha_0 = \beta_0 = 1$. Then (A.11) implies as $\kappa \to \infty$

$$\begin{cases} N_l &= \mathrm{e}^{\mathrm{i}(\kappa - \frac{l\pi}{2} + \mathrm{i}\beta_1)} \left(1 + \mathrm{i}\beta_2\kappa^{-1} + \mathcal{O}(\kappa^{-2})\right) \\ &\quad + \left((\beta_1 - \alpha_1)\kappa^{-1} + \mathcal{O}(\kappa^{-2})\right) \sin(\kappa - \frac{l\pi}{2} + \mathrm{i}\beta_1) \\ D_l &= \mathrm{e}^{-\mathrm{i}(\kappa - \frac{l\pi}{2} + \mathrm{i}\beta_1)} \left(1 - \mathrm{i}\beta_2\kappa^{-1} + \mathcal{O}(\kappa^{-2})\right) \\ &\quad - \left((\beta_1 - \alpha_1)\kappa^{-1} + \mathcal{O}(\kappa^{-2})\right) \sin(\kappa - \frac{l\pi}{2} + \mathrm{i}\beta_1). \end{cases} \tag{A.12}$$

Along the real axis all the exponential terms contribute, and the quotient is

$$\rho^{\mathrm{c}}_{\tau l} = \mathrm{e}^{\mathrm{i}2(\kappa - \frac{l\pi}{2} + \mathrm{i}\beta_1)} \left(1 + \mathrm{i}2\beta_2\kappa^{-1} + (\beta_1 - \alpha_1)\kappa^{-1} \sin(2\kappa - l\pi + \mathrm{i}2\beta_1) + \mathcal{O}(\kappa^{-2})\right). \tag{A.13}$$

In the upper half-plane as $\kappa \hat{\to} \infty$, the term $\mathrm{e}^{\mathrm{i}2\kappa}$ is exponentially small and the main contribution comes from terms of the form $\mathrm{e}^{-\mathrm{i}2\kappa}$. Therefore, the dominant contribution is given by

$$\begin{aligned} \rho^{\mathrm{c}}_{\tau l} = \mathrm{e}^{\mathrm{i}2(\kappa - \frac{l\pi}{2} + \mathrm{i}\beta_1)} \Big[1 + \mathrm{i}2\beta_2\kappa^{-1} + (\beta_1 - \alpha_1)\kappa^{-1} \sin(2\kappa - l\pi + \mathrm{i}2\beta_1) \\ + \mathcal{O}(\kappa^{-2}) \sin(\kappa - \frac{l\pi}{2} + \mathrm{i}\beta_1)\mathrm{e}^{-\mathrm{i}(\kappa - \frac{l\pi}{2} + \mathrm{i}\beta_1)} + \mathcal{O}(\kappa^{-2})\Big] \\ = \mathrm{i}\frac{\beta_1 - \alpha_1}{2ka} + \mathcal{O}((ka)^{-2}) \end{aligned} \tag{A.14}$$

where $\kappa = ka$ has been inserted.

References

[1] M. Abramowitz and I. A. Stegun, editors. *Handbook of Mathematical Functions.* Applied Mathematics Series No. 55. National Bureau of Standards, Washington D.C., 1970.

[2] G. B. Arfken and H. J. Weber. *Mathematical Methods for Physicists.* Academic Press, New York, fifth edition, 2001.

[3] A. Bernland, M. Gustafsson, and S. Nordebo. Physical limitations on the scattering of electromagnetic vector spherical waves. Technical Report LUTEDX/(TEAT-7194)/1-24/(2010), Lund University, Department of Electrical and Information Technology, P.O. Box 118, S-221 00 Lund, Sweden, 2010. `http://www.eit.lth.se`.

[4] A. Bernland, A. Luger, and M. Gustafsson. Sum rules and constraints on passive systems. Technical Report LUTEDX/(TEAT-7193)/1-31/(2010), Lund University, Department of Electrical and Information Technology, P.O. Box 118, S-221 00 Lund, Sweden, 2010. `http://www.eit.lth.se`.

[5] C. R. Brewitt-Taylor. Limitation on the bandwidth of artificial perfect magnetic conductor surfaces. *Microwaves, Antennas & Propagation, IET*, **1**(1), 255–260, 2007.

[6] L. J. Chu. Physical limitations of omni-directional antennas. *Appl. Phys.*, **19**, 1163–1175, 1948.

[7] P. L. Duren. *Theory of H^p Spaces*. Dover Publications, New York, 2000.

[8] R. M. Fano. Theoretical limitations on the broadband matching of arbitrary impedances. *Journal of the Franklin Institute*, **249**(1,2), 57–83 and 139–154, 1950.

[9] W. Geyi. Physical limitations of antenna. *IEEE Trans. Antennas Propagat.*, **51**(8), 2116–2123, August 2003.

[10] M. Gustafsson and D. Sjöberg. Sum rules and physical bounds on passive metamaterials. *New Journal of Physics*, **12**, 043046, 2010.

[11] M. Gustafsson, C. Sohl, and G. Kristensson. Physical limitations on antennas of arbitrary shape. *Proc. R. Soc. A*, **463**, 2589–2607, 2007.

[12] M. Gustafsson, C. Sohl, and G. Kristensson. Illustrations of new physical bounds on linearly polarized antennas. *IEEE Trans. Antennas Propagat.*, **57**(5), 1319–1327, May 2009.

[13] M. Gustafsson. Sum rule for the transmission cross section of apertures in thin opaque screens. *Opt. Lett.*, **34**(13), 2003–2005, 2009.

[14] M. Gustafsson and S. Nordebo. Bandwidth, Q factor, and resonance models of antennas. *Progress in Electromagnetics Research*, **62**, 1–20, 2006.

[15] M. Gustafsson and S. Nordebo. Characterization of MIMO antennas using spherical vector waves. *IEEE Trans. Antennas Propagat.*, **54**(9), 2679–2682, 2006.

[16] M. Gustafsson, C. Sohl, C. Larsson, and D. Sjöberg. Physical bounds on the all-spectrum transmission through periodic arrays. *EPL Europhysics Letters*, **87**(3), 34002 (6pp), 2009.

[17] J. E. Hansen, editor. *Spherical Near-Field Antenna Measurements*. Number 26 in IEE electromagnetic waves series. Peter Peregrinus Ltd., Stevenage, UK, 1988. ISBN: 0-86341-110-X.

[18] A. Hujanen, J. Holmberg, and J. C.-E. Sten. Bandwidth limitations of impedance matched ideal dipoles. *IEEE Trans. Antennas Propagat.*, **53**(10), 3236–3239, 2005.

[19] J. D. Jackson. *Classical Electrodynamics*. John Wiley & Sons, New York, third edition, 1999.

[20] H. M. Nussenzveig. *Causality and dispersion relations.* Academic Press, London, 1972.

[21] F. W. J. Olver. *Asymptotics and special functions.* A K Peters, Ltd, Natick, Massachusetts, 1997.

[22] A. Papoulis. *The Fourier integral and its applications.* McGraw-Hill, Inc., New York, 1962.

[23] K. N. Rozanov. Ultimate thickness to bandwidth ratio of radar absorbers. *IEEE Trans. Antennas Propagat.*, **48**(8), 1230–1234, August 2000.

[24] C. Sohl and M. Gustafsson. A priori estimates on the partial realized gain of Ultra-Wideband (UWB) antennas. *Quart. J. Mech. Appl. Math.*, **61**(3), 415–430, 2008.

[25] C. Sohl, M. Gustafsson, and G. Kristensson. Physical limitations on broadband scattering by heterogeneous obstacles. *J. Phys. A: Math. Theor.*, **40**, 11165–11182, 2007.

[26] C. Sohl, M. Gustafsson, and G. Kristensson. Physical limitations on metamaterials: Restrictions on scattering and absorption over a frequency interval. *J. Phys. D: Applied Phys.*, **40**, 7146–7151, 2007.

[27] J. A. Stratton. *Electromagnetic Theory.* McGraw-Hill, New York, 1941.

[28] H. L. Thal. Exact circuit analysis of spherical waves. *IEEE Trans. Antennas Propagat.*, **26**(2), 282–287, March 1978.

[29] M. C. Villalobos, H. D. Foltz, and J. S. McLean. Broadband matching limitations for higher order spherical modes. *IEEE Trans. Antennas Propagat.*, **57**(4), 1018–1026, 2009.

[30] M. C. Villalobos, H. D. Foltz, J. S. McLean, and I. S. Gupta. Broadband tuning limits on UWB antennas based on Fano's formulation. In *Proceedings of Antennas and Propagation Society International Symposium 2006*, pages 171–174, 2006.

[31] J. Volakis, C. C. Chen, and K. Fujimoto. *Small Antennas: Miniaturization Techniques & Applications.* McGraw-Hill, New York, 2010.

[32] H. A. Wheeler. The wide-band matching area for a small antenna. *IEEE Trans. Antennas Propagat.*, **31**, 364–367, 1983.

[33] M. Wohlers and E. Beltrami. Distribution theory as the basis of generalized passive-network analysis. *IEEE Transactions on Circuit Theory*, **12**(2), 164–170, 1965.

[34] A. D. Yaghjian and S. R. Best. Impedance, bandwidth, and Q of antennas. *IEEE Trans. Antennas Propagat.*, **53**(4), 1298–1324, 2005.

[35] D. Youla, L. Castriota, and H. Carlin. Bounded real scattering matrices and the foundations of linear passive network theory. *IRE Transactions on Circuit Theory*, **6**(1), 102–124, 1959.

[36] A. H. Zemanian. *Distribution theory and transform analysis: an introduction to generalized functions, with applications.* McGraw-Hill, New York, 1965.